Articles

Biochemical Evolution of DNA Polymerase η: Properties of Plant, Human, and Yeast Proteins[†]

Peter D. Hoffman,[‡] Marc J. Curtis,[‡] Shigenori Iwai,[§] and John B. Hays*,[‡]

Department of Environmental and Molecular Toxicology, Oregon State University, Corvallis, Oregon 97331-7301, and Graduate School of Engineering Science, Osaka University, 1-3 Machikaneyama, Toyonaka, Osaka 560-8531, Japan

Received August 30, 2007; Revised Manuscript Received December 20, 2007

ABSTRACT: To assess how evolution might have biochemically shaped DNA polymerase η (Polη) in plants, we expressed in *Escherichia coli* proteins from *Arabidopsis thaliana* (At), humans (Hs), and the yeast *Saccharomyces cerevisiae* (Sc), purified them to near homogeneity, and compared their properties. Consistent with the multiple divergent amino acids within mostly conserved polymerase domains, the polymerases showed modest, appreciable, and marked differences, respectively, in salt and temperature optima for activity and thermostability. We compared abilities to extend synthetic primers past template cyclobutane thymine dimers (T[CPD]T) or undamaged T-T under physiological conditions (80–110 mM salt). Specific activities for "standing-start" extension of synthetic primers ending opposite the second template nucleotide 3′ to T-T were roughly similar. During subsequent "running-start" insertions past T-T and the next 5′ ($N + 1$) nucleotide, AtPolη and HsPolη appeared more processive, but DNA sequence contexts strongly affected termination probabilities. Lesion-bypass studies employed four different templates containing T[CPD]Ts, and two containing pyrimidine (6-4′)-pyrimidinone photoproducts ([6-4]s). AtPolη made the three successive insertions [opposite the T[CPD]T and ($N + 1$) nucleotides] that define bypass nearly as well as HsPolη and somewhat better than ScPolη. Again, sequence context effects were profound. Interestingly, the level of insertion opposite the ($N - 1$) nucleotide 3′ to T[CPD]T by HsPolη and especially AtPolη, but not ScPolη, was reduced (up to 4-fold) relative to the level of insertion opposite the ($N - 1$) nucleotide 3′ to T-T. Evolutionary conservation of efficient T[CPD]T bypass by HsPolη and AtPolη may reflect a high degree of exposure of human skin and plants to solar UV-B radiation. The depressed ($N - 1$) insertion upstream of T[CPD]T (but not T-T) may reduce the extent of gratuitous error-prone insertion.

Recent years have seen a dramatic increase in the list of distinct eukaryotic DNA polymerases, well beyond the five previously identified with semiconservative DNA replication and postexcision DNA repair synthesis (for recent reviews, see ref *1*). Most "new" polymerases appear to be specialized for particular activities. Recognition of the remarkable abilities of a subset of specialized DNA polymerases to synthesize DNA past template lesions that block replicative polymerases has revolutionized our understanding of cellular responses to such lesions.

Although the biochemical activities of the respective translesion synthesis polymerases (TLS polymerases) vary widely, they jointly differ from replicative polymerases in several important respects. First, their open substrate binding pockets allow them to accommodate even bulky and highly distorting template lesions and to insert as nucleotides opposite them (surprisingly frequently) the formal Watson–Crick complements (*2*). Second, their lack of 3′-exonucleolytic proofreading allows nucleotide:lesion mispairs to be extended. As expected, both of these properties cause TLS polymerases to copy undamaged DNA much less accurately than replicative polymerases. Error-prone insertion opposite lesions may be an acceptable price to pay for timely replication of damaged DNA. Gratuitous mutation by inaccurate copying of undamaged DNA by TLS polymerases would seem to be minimized by their third common property, highly nonprocessive synthesis.

Many TLS polymerases share motifs that define a new group of DNA polymerases, the Y family, the members of which extend across all three kingdoms of life (*3*). Prominent in the Y family are the polymerase η orthologs, found in virtually all eukaryotes. *Saccharomyces cerevisiae* polymerase η (ScPolη)[1] was identified to be the product of the *RAD30* gene (*4*), while human polymerase

[†] Supported by Grant MCB 03455061 to J.B.H. from the National Science Foundation.

* To whom correspondence should be addressed. E-mail: haysj@science.oregonstate.edu. Phone: (541) 737-1778. Fax: (541) 737-0497.

[‡] Oregon State University.

[§] Osaka University.

[1] Abbreviations: CPD, cyclobutane pyrimidine dimer; [6-4], 6-4 pyrimidine-pyrimidinone photoproduct; Polη, DNA polymerase η; AtPolη, *Arabidopsis thaliana* Polη; ScPolη, *Saccharomyces cerevisiae* Polη; HsPolη, human Polη.

10.1021/bi701781p CCC: $40.75
Published on Web 03/27/2008

η (HsPolη) was found to be the protein deficient in UV-sensitive xeroderma pigmentosum variant (XP-V) patients (*5*). XP-V cells remove the predominant photoproducts induced in DNA by UV radiation, *cis syn* cyclobutane pyrimidine dimers (CPDs), at normal (slow) rates. Nevertheless, these cells are abnormally slow to complete DNA replication after UV irradiation and exhibit elevated levels of UV mutagenesis (*6*). This phenotype is perfectly consistent with the reported abilities of HsPolη (and ScPolη) to synthesize DNA past T-T CPDs (T[CPD]Ts) much more efficiently than replicative polymerases, with relatively low error rates of $10^{-3}-10^{-2}$ (*7*).

The remarkable T[CPD]T bypass by Polη proteins has motivated the suggestion that various TLS polymerases are specialized for particular cognate lesions (*1*). However, Polη also synthesizes DNA past 8-oxoguanine more accurately than replicative polymerases (*8*), and all TLS polymerases show at least some bypass of broad (but far from unlimited) ranges of lesions (*3*). We suggest that even in a particular class of orthologs, evolution has shaped particular polymerases to synthesize DNA past one or more lesions commonly encountered by the respective organisms with efficiency and accuracy, but also to retain some versatility. We reasoned that CPDs would be frequently encountered by green plants, since they are heavily exposed to solar UV-B radiation. To test this hypothesis, we separately expressed in *Escherichia coli* C-terminally His_6-tagged yeast, human, and *Arabidopsis* Polη (AtPolη) proteins and purified them to near homogeneity. Biochemically, AtPolη and HsPolη prove to resemble one another more than either resembles ScPolη. Both bypass CPDs efficiently, but both show an unexpectedly reduced level of insertion opposite the undamaged template nucleotides immediately 3′ to T[CPD]T. In all cases, the DNA sequences surrounding T[CPD]T strongly affect Polη activity.

MATERIALS AND METHODS

Plasmids Encoding Polη-(His_6) Protein. To obtain *Arabidopsis AtPOLH* (AtPolη) cDNA, an RNeasy plant mini kit (Qiagen) was used to extract mRNA from ~100 14-day seedlings. A Marathon (Clontech) cDNA amplification kit was used according to the manufacturer's protocols to prepare an initial cDNA using AMV reverse trancriptase and to determine 5′ and 3′ end sequences by rapid amplification of cDNA ends (RACE). The coding sequence corresponded exactly to the annotated database (TAIR) sequence. It was cloned in frame into the Novagen pET21A *E. coli* expression vector as follows. AtPolη primers encoding sites (underlined) for restriction endonucleases *Nde*I (NdeI) and *Xho*I (XhoI), 5′CATATGCCGGTAGCGAGACCGGAAG and 5′CTCGAGCCATCTATTCAATGGTGGAAAATGAGC, respectively, were used to PCR-amplify the AtPolη cDNA template. The product was cloned into plasmid pCRII using topoisomerase-mediated ligation according to the manufacturer's protocol (Invitrogen). Intermediate vectors were digested with NdeI and XhoI, and the gel-purified AtPolη fragment was inserted into the NdeI and XhoI sites of pET21A to fuse His_6 to the C-terminus, using standard techniques. The AtPolη-encoding sequence in the resulting construct (pET21-AtPolη-His) was verified by determining the complete sequence of both strands. We employed a QuikChange (Stratagene) kit, according to the manufacturer's protocols, to similarly generate a plasmid encoding an AtPolη catalytic mutant [pET21-AtPolη(DE120-121AA)-His], using mutagenic primers 5′GAGAGGGCTTCGATT*GCTGCA*GTGTATCTTGACCTC and 5′GAGGTCAAGATACAC*TGCAGC*AATCGAAGCCCTCTC [the italicized mutant codons overlap a recognition site (CTGCAG) for restriction endonuclease *Pst*I (*Pst*I) which allows rapid screening for mutagenized plasmids]. pET21A-based expression vectors for wt (pET21-XPV-His) and catalytically inactivated human polymerase η (HsPolη), designated pET21-XPV(DE115–116AA)-His, were kind gifts of F. Hanaoka. Z. Wang generously provided pEGUh6-RAD30 (*9*) which encodes ScPolη. The ScPolη coding sequence from pEGUh6-RAD30 was PCR-amplified using primers 5′CATATGTCAAAATTTACTTGGAAGGAGTTG and 5′CTCGAGTCCTTTTTTTCTTGTAAAAAATGATAAGATGTTTTTGG (NdeI and XhoI restriction sites underlined, respectively), and the product was cloned into the NdeI and XhoI sites of pET21A, yielding pET21-ScPolη-His. Its DNA sequence was verified. A plasmid expressing an active-site ScPolη mutant [pET21-ScPolη(DE155–156AA)-His] was created from pET21-ScPolη-His using primers 5′GAAAGGGCGAGTATT*GCTGCA*GTATTTCTTGATTTG and 5′CAAATCAAGAAATAC*TGCAGC*AATACTCGCCCTTTC to introduce overlapping codon/anticodon changes (italicized) overlapping a *Pst*I site, as described above for AtPolη(DE120–121AA). Product plasmids were screened for *Pst*I sensitivity, and sequences were verified. For each pET21A-derived plasmid, expression driven by the T7 RNA polymerase (derepressed by IPTG addition) yields a C-terminally His_6-tagged protein.

Overexpression and Purification of Polη Proteins. Polη-expressing plasmids were transformed into competent *E. coli* strain BL21-λde3 Codon+ (Stratagene) using the manufacturer's protocol. Varying aliquots of transformation mixtures were plated on LB plates (1% tryptone, 0.5% yeast extract, 170 mM NaCl, and 1.5% agar) also containing 35 μg/mL chloramphenicol (Cm) and 100 μg/mL ampicillin (Amp) and then incubated overnight at 37 °C. Plates with ~50 individual colonies were flooded with 5 mL each of sterile LB and 50% glycerol. Colonies were detached by mechanical agitation with a sterile glass spreading rod. The resulting slurry was aseptically transferred to a sterile 15 mL centrifuge tube and vortexed briefly to ensure uniformity. Aliquots (1 mL) were transferred to sterile cryogenic storage tubes and stored at −80 °C. For typical protein purifications, aliquots were thawed on ice and the pooled transformant stock was diluted 1:100 into CircleGrow (Bio101) medium containing Amp (100 μg/mL) and Cm (35 μg/mL). Cultures were grown overnight at 30 °C, then diluted 10-fold with the same culture medium, and grown for an additional 4 h at 37 °C until the A_{600} was ~0.6. Cultures were placed on liquid ice for 20 min; then IPTG was added to a final concentration of 0.5 mM, and cultures were incubated for 40 h at 12 °C. The use of pooled fresh transformants and long-duration low-temperature induction proved critical for large yields of full-length active protein and could be scaled up to at least 2−3 L of culture without significant loss of induction.

Cells were centrifuged for 10 min at 7000*g*, rinsed in resuspension buffer [10 mM KPO_4 (pH 7.4), 10% glycerol, and 300 mM NaCl], centrifuged again, and resuspended in 0.15 volume of resuspension buffer containing protease

inhibitors [phenylmethanesulfonyl fluoride (PMSF), 1 μL of saturated 2-propanol solution per 1.5 mL of lysate; Roche complete EDTA-free cocktail, 1× as recommended for the lysate volume]. All subsequent manipulations were performed on ice or at 4 °C. Lysate mixtures were treated with powdered lysozyme (100 mg mixed thoroughly per 50 mL of resuspension buffer) for 10 min and then subjected to ultrasonic radiation six times for 15 s; the tip and solution were cooled after each treatment. Lysates were centrifuged at 15000*g* for 15 min, transferred to clean tubes, and again centrifuged at 15000*g* for 15 min. Supernatants were mixed with 1.0 mL of Talon (Co^{2+}) resin slurry {50% w/v; equilibrated in binding buffer [10 mM KPO_4 (pH 7.4), 10% glycerol, 300 mM NaCl, and 5 mM imidazole]} per 50 mL lysate volume and incubated with constant mixing for 30 min. Loose resin pellets were recovered by centrifugation at 400*g*, and recovered resin was pooled and transferred to a SnapCap disposable column (Bio-Rad). The lysate supernatant, followed by 30 column volumes of binding buffer (containing 10 mM imidazole), was passed through the column at a rate of 5 mL/min using a peristaltic pump. Protein was eluted (gravity flow) by four to five sequential applications of 1 mL of binding buffer containing 300 mM imidazole. Fractions (typically two) containing significant Polη protein [as established by polyacrylamide gel electrophoresis in 1% sodium dodecyl sulfate (SDS−PAGE) and Coomassie Brilliant Blue staining] were pooled and applied to a Sephadex G-25 desalting column equilibrated in column buffer [50 mM KPO_4 (pH 7.4), 1 mM EDTA, 1 mM β-mercaptoethanol, and Roche protease inhibitors; see above]. During elution with 50 mL of this buffer, 0.5 mL fractions were collected and their A_{280} was monitored. Fractions showing significant A_{280} were analyzed by SDS−PAGE. Those containing Polη protein were pooled and applied to a 1 mL Heparin HiTrap column (Pharmacia) equilibrated in column buffer. The column was washed with column buffer until the fractions showed no detectable UV absorbance (typically 20 mL) and then eluted with a 50 mL gradient from 0 to 1 M KCl in column buffer. Fractions (1 mL) containing Polη were identified and pooled. Peak protein fractions typically eluted at ∼300 mM KCl. If significant contaminating protein was detected (by SDS−PAGE) in the pooled fractions, the fractions were diluted 1:5 in column buffer and applied to an identical Heparin column, which was washed as described above and eluted with 0.1 to 1 M KCl in column buffer. Final protein preparations were typically >98% pure (Figure 1). Sterile glycerol was added to 25% (v/v) bovine serum albumin (DNase-free) to a final concentration of 1 mg/mL and dithiothreitol to 1 mM (storage buffer). Aliquots of pooled protein, typically 20 μL, were flash-frozen in liquid N_2 and stored at −80 °C. Individual aliquots were used only once. The three mutant polymerases, AtPolη(DE120–121AA),HsPolη(DE115–116AA),andScPolη (DE155–156AA), were purified by essentially identical procedures.

DNA Substrates. R. Woodgate (National Institute of Child Health and Human Development, National Institutes of Health, Bethesda, MD) kindly provided 48-nucleotide oligomers containing T[CPD]T photoproducts at defined positions (contexts *I* and *II*). These had been synthesized using T[CPD]T phosphoramadite subunits synthesized by Glen Research. The 20-nucleotide oligomers containing T[CPD]T

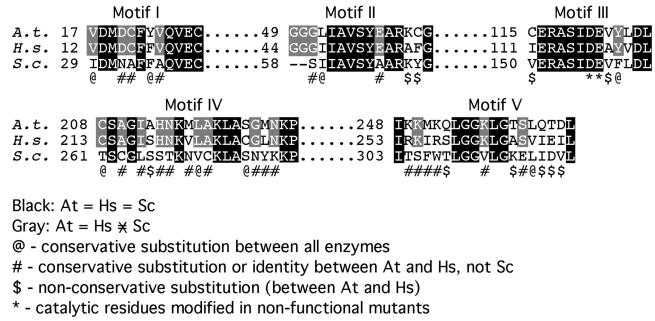

FIGURE 1: Amino acid sequences in conserved DNA polymerase η motifs. Sequences of *Arabidopsis thaliana* (A.t.), human (H.s.), and *S. cerevisae* (S.c.) polymerase η proteins have been partially aligned elsewhere (*23*). We show here amino acids that are identical (or only conserved) in all three enzymes, amino acids that are identical (or only conserved) between AtPolη and HsPolη but not ScPolη, and positions of nonconservative substitution between AtPolη (at times conserved between one or the other and ScPolη). Asterisks indicate catalytic residues modified in nonfunctional versions of all three polymerases.

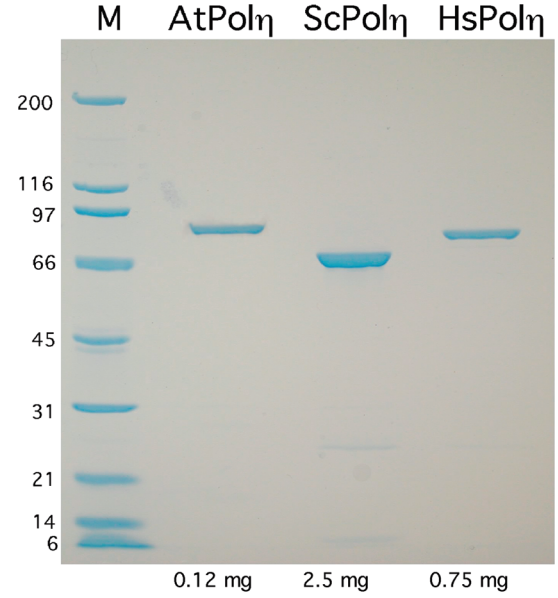

FIGURE 2: Purity of Polη proteins. Samples (roughly 5 μg) of indicated proteins were subjected to denaturing electrophoresis in a 4 to 15% polyacrylamide gel by standard techniques and stained with Coomassie Blue. Yields (per initial liter of protein-overexpressing *E. coli* culture) of proteins purified as described in Overexpression and Purification of Polη Proteins are shown. M, protein molecular mass markers (kilodaltons).

and T[6-4]T in contexts *III* and *IV* were synthesized as previously described (*10*). These were extended to 31 nucleotides by attaching to their 3′ ends the same 11-nucleotide oligomers (italics below) by standard scaffolded ligation. Photoproduct sites are underlined: context *I*, 5′TCG ATACTGGTACTAATGATTAACGAATTAAG-CACGTCCGTACCATCG3′; context *II*, 5′TCGATACTG-GTACTAATGATTAACGAGTTAAGCACGTCCGTACCATCG3′; context *III*, 5′CCTACGCGAATTCGGCATCC*AAGCACGTC-CG3′*; context *IV*, 5′CCTACGCAAATTTGGCATCC*AAG-CACGTCCG3′*. Complementary primers terminating at defined positions relative to template strands (Figure 3) were synthesized by MWG Biotech; these were purified and then 5′-end-labeled using [^{32}P]ATP (Perkin-Elmer) and T4 polynucleotide kinase (PNK) (New England Biolabs) under

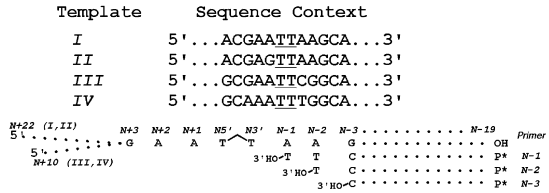

FIGURE 3: For any position (template nucleotide) N after the nucleotide opposite the original primer end, the termination probability equals the intensity of the band corresponding to the extension product ending opposite N divided by the summed intensities of bands corresponding to all extension products N and larger. For example, for extension of any of the three synthetic primers ($N - 1$, $N - 2$, and $N - 3$) annealed to template I, Pr{$N3'$ termination} = [$N3'$ band]/[$N3' + N5' + (N + 1) + ...$ ($N + 22$ or $N + 10$) bands (depending on the length of the template strand)]. For any position N at least two nucleotides after the synthetic primer end, the insertion probability equals the summed intensity of all bands corresponding to extension products ending opposite N or longer, divided by the intensities of the $N - 1$ band plus all further extension products. With template I and primer $N - 2$, for example, Pr{$N3'$ insertion} = [$N3' + N5' + (N + 1) + ...$ ($N + 22$) bands]/[$(N - 1) + N3' + N5' + (N + 1) + ...$ ($N + 22$) bands]. Note that, for example, Pr{$N - 1$ termination} = 1 − Pr{$N3'$ insertion}.

conditions recommended by the manufacturer. Primer/template mixtures (molar ratio of 1:1.2) were heated to 85 °C in PNK buffer [70 mM Tris-HCl (pH 7.6), 10 mM $MgCl_2$, and 5 mM DTT] in a 2 L water bath, and the bath was allowed to cool to room temperature. We typically added 0.25 μL aliquots of annealed duplexes (300 fmol) directly to 20 μL primer-extension reaction mixtures.

Extension of Defined DNA Primers past Template Photoproducts under Standard Reaction Conditions. These were essentially as described by Kunkel and co-workers (*11*), except that we used salt concentrations and temperatures that were optimal for each polymerase. Standard primer-extension buffer contained 40 mM Tris (pH 8.0), 5 mM $MgCl_2$, 10 mM dithiothreitol, 100 μM dNTPs, and 1 mg/mL bovine serum albumin. Special additions are noted below. Typical time-course analyses employed 1500 fmol of primer−template DNA and 15−37.5 fmol of polymerase in reaction volumes of 100 μL. Concentrations of the three Polη proteins were empirically adjusted to yield similar reaction rates at the standard optimal reaction temperatures: AtPolη, 22 °C; ScPolη, 30 °C; HsPolη, 37 °C. At time zero, 75 μL of cocktail containing 1.33× concentrated primer-extension buffer with DNA substrate was mixed with 25 μL of diluted polymerase and incubated. At desired times, 10 μL aliquots were removed and mixed with an equal volume of stop buffer (100% formamide, 25 mM EDTA, 0.06% bromophenol blue, and 0.02% xylene cyanol) and incubated at 95 °C for 5 min, and a 2.5 μL aliquot was analyzed on a standard sequencing gel (8 M urea and 12% polyacrylamide). After gels were dried, band intensities were determined by phosphorimaging and analysis using ImageQuant (Molecular Dynamics). None of the preparations of the three mutant polymerases, AtPolη (DE120–121AA), HsPolη(DE115–116AA), and ScPolη (DE155–156AA), processed in parallel to equivalent purity, exhibited detectable primer-extension activity. Thus, none of our observations can be attributed to trace levels of *E. coli* DNA polymerases.

Determination of Salt Optima. Standard reaction mixtures were augmented with 20–120 mM KCl in 10 mM increments. The efficiency of undamaged ($N - 1$) context I primer/templates mixtures was analyzed after a 4 min incubation at 25 °C.

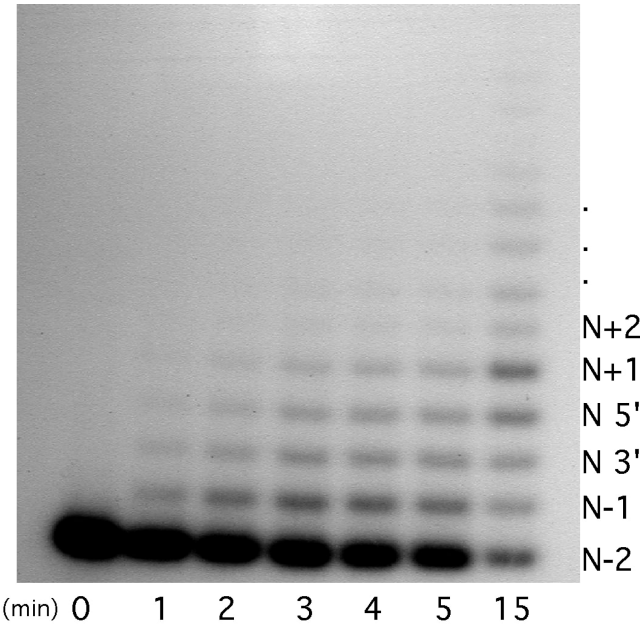

FIGURE 4: Single-hit extension of primers paired with undamaged templates. Running-start extension of an ($N - 2$)-ended synthetic primer paired with a context I template (150 nM) by AtPolη (7.5 nM) was analyzed as described in Materials and Methods. Under these single-hit kinetics, intensities of extension products ending opposite template nucleotides $N - 1$, $N3'$, ..., remained constant relative to one another at times up to 5 min, as unextended-primer ($N - 2$) bands diminished.

Determination of Temperature Optima. Standard reaction mixtures containing the KCl concentrations determined to be optimum for each polymerase were incubated at 15, 22, 27, 30, 37, and 45 °C. Extension efficiency was scored after 4 min. Unless otherwise indicated, all other primer-extension reactions were performed under the optimal conditions for each polymerase: AtPolη, 80 mM KCl and 22 °C; ScPolη, 90 mM KCl and 30 °C; HsPolη, 110 mM KCl and 37 °C.

Measurement of Heat Lability. Each polymerase was first diluted in primer-extension buffer (without dNTPs) to enzyme concentrations separately determined to yield single-hit kinetics for at least 4 min (see below). Mixtures were incubated at 15, 20, 25, 30, 37, and 45 °C, and aliquots were removed at various times, augmented with KCl to the respective optimal concentrations, and held on ice. These samples were analyzed for extension at a single 4 min time point as described in Determination of Salt Optima.

Single-Hit Kinetics. Enzyme stocks were diluted in storage buffer through 16 sequential 2-fold dilutions to a final concentration of ∼1:32000 and the intensities of primer-extension products after a 4-min extension analyzed for each dilution (Figure 4 shows representative primer-extension products). "Single-hit kinetics" are said to prevail over the dilution range where the product bands show the same relative ratios as their absolute intensities decrease. This titration was used to establish a range over which single-hit kinetics (constant band ratios) prevailed for at least three successive dilutions. From these, a single enzyme concentration was selected at which single-hit kinetics prevailed over at least three successive time points (typically 2, 3, and 4 min). Ratios typically remained constant up to times at which

>40% of the total substrate was extended, at which point second rounds of extension became apparent.

Analysis of Primer-Extension Data. Probabilities of termination, insertion, and complete lesion bypass were determined as described by Kokoska et al. (*11*), with modification for a two-nucleotide lesion (Figure 3). In general, for a primer with a terminal (3′-OH) nucleotide opposite template nucleotide *N*, the *N* termination probability equals the intensity of the *N*-product band divided by the sum of the intensities of the bands corresponding to the *N* product and all further extension products ($N + 1$, $N + 2$, ...). The $N + 1$ insertion probability equals the summed intensities of all bands for extension products of length *N* or greater divided by the intensities of the $N - 1$ band and all further extension products ($N + 1$, $N + 2$, ...). Thus, *N* insertion probability $= 1 -$ ($N - 1$ termination probability). The special case of $N + 1$ insertion opposite the first undamaged template nucleotide 3′ to an *N*5′*N*3′ lesion is sometimes termed "extension" for that lesion. The lesion bypass probability equals the summed intensities of bands for $N + 1$ and longer products ($N + 2$, $N + 3$, ...) divided by the summed intensities of $N - 1$ and all longer product (*N*3′, *N*5′, $N + 1$, ...) bands (see Figure 3).

RESULTS

Evolution of Biochemical Properties. The AtPolη, HsPolη, and ScPolη proteins exhibit several nonconservative changes in their mostly similar DNA polymerase motifs I−V (Figure 1), as well as nonconservative changes elsewhere. To determine whether these changes might affect their biochemical properties, we expressed the respective His_6-tagged polymerases under identical conditions in *E. coli* and used very similar protocols to purify them to near (>98%) homogeneity (Figure 2). To the best of our knowledge, this is the first report of large yields of full-length recombinant HsPolη from bacteria. It proved important to prepare fresh initial inocula of bacteria transformed with expression vectors, by washing colonies directly off selection plates and suspending roughly 50 colonies in 25% glycerol and storing them at −80 °C. (We typically observed poor induction of expression in cultures started from single colonies picked off selection plates, especially after several passages of bacteria on plates.) After overnight growth at 30 °C and subculturing at 37 °C, subsequent induction and prolonged expression were carried out at 12 °C. Although yields of purified HsPolη (0.75 mg/L of culture) and especially ScPolη (2.5 mg/L) were quite robust, yields of AtPolη were only 0.12 mg/L. At least some loss of AtPolη seems to be due to proteolytic degradation during expression and perhaps purification (data not shown).

Table 1 compares some properties of the three polymerases. Consistent with the differences in primary structure, there are appreciable differences in activity−salt profiles (Figure 1 of the Supporting Information) and greater differences in temperature optima. Interestingly, the optimum temperatures roughly correspond to those at which *Arabidopsis*, yeast cells, and human cells are typically grown in the laboratory, and the optimum salt concentrations would be considered roughly "physiological". The striking differences in thermal stability (Table 1, column 5) did not correlate with the temperature optima (column 3). The specific activities (femtomoles of undamaged primer/template mixtures extended per minute per picomole of polymerase) for standing-start $N - 1$ insertions using ($N - 2$)-ended synthetic primers (see definition below) were similar, particularly when approximately corrected for reaction temperatures (Table 1, column 4, values in parentheses). Thus, the fractions of inactive polymerase (if any) in the respective preparations appeared to be similar. We next compared enzymatic properties.

Table 1: Properties of Polymerase η Proteins

polymerase	activity optima[a] [salt] (mM)	activity optima[a] temp[d] (°C)	specific[b] activity	half-life[c] at 45 °C (min)
AtPolη	80	22	6.1 (10)	2.5
HsPolη	110	37	21.0 (15)	7.0
ScPolη	90	30	9.7 (10)	1.0

[a] Total extension of primers paired with undamaged template (context AATTAA) was assessed under single-hit conditions in extension buffer containing KCl at varying concentrations (range of 20–120 mM, 10 mM increments) at 30 °C. Optimal 30 °C salt conditions for each enzyme for measurements of activity at 22, 30, and 37 °C. Salt optima were reconfirmed at optimal temperatures for each enzyme. Specific activities were determined at 22, 30, and 37 °C for At, Sc, and Hs enzymes, respectively, at their optimal salt concentrations. [b] Extension of primers opposite undamaged template (context AATTAA; concentration of 30 nM) was assessed under single-hit conditions at salt and temperature optima for the respective polymerases (concentration of 1–3 nM). Initial rates were determined from data obtained for (typically) incubation for 1−3 min. Specific activity equals femtomoles of primer extended per minute per picomole of polymerase. Parentheses enclose activities roughly corrected for the effect of temperature on reaction, assuming Q_{10} of 2. [c] Polymerases were diluted in storage buffer to equal concentrations, incubated at 45 °C for various times, and then diluted 16-fold and assayed as described for specific activity. [d] Relative activities at 22, 30, and 37 °C (compared to activities at indicated temperature optima) were as follows: At (1.0), 0.65, 0.15; Hs 0.6, 0.75, (1.0); Sc 0.95, (1.0), 0.87, respectively.

Extension of Undamaged Primer−Templates. We used the primer-extension techniques of Goodman and co-workers (*12*) and data analyses described by Kunkel and co-workers (*11*) to compare in detail the three polymerases. The templates contained thymine-thymine photoproducts (typically T[CPD]T) or normal T-T dinucleotides at positions designated here as *N*5′ and *N*3′, embedded in four different sequence contexts (Figure 3, top panel). Template nucleotides extending from the photoproducts in the 5′ and 3′ directions are, respectively, designated $N + 1$, $N + 2$, ... and $N - 1$, $N - 2$, ... (Figure 3, bottom panel). The three chemically synthesized primers employed in various experiments are designated by the template nucleotides opposite the primer 3′-OH nucleotides $N - 1$, $N - 2$, and $N - 3$ (Figure 3, bottom panel). Standing-start insertion is defined as addition of the first nucleotide to any of these synthetic primers, insertion opposite template $N - 1$ for $N - 2$ primers, for example. Successive additions of the second, third, etc., nucleotides are designated "running-start" insertions, e.g., *N*3′, *N*5′, $N + 1$ ... for $N - 2$ primers. [In some previous reports, synthetic primers were named relative to the photoproduct position, as standing-start ($N - 1$ here) or running-start ($N - 2$ and $N - 3$ here).]

To compare intrinsic polymerization biochemistry (in the absence of cofactors such as the PCNA clamp and the ssDNA-binding protein RPA), we assessed abilities of the polymerases to extend primers under single-hit conditions: high DNA to polymerase molar ratios (typically 20–50:

1) and short incubation times (1–6 min). We first decreased polymerase concentrations (at fixed DNA concentrations) until primer-extension patterns at early times showed similar band intensities relative to one another (but decreasing absolute band intensities), indicative of single rounds of primer extension (Figure 2 of the Supporting Information). The relative intensities of the respective extension products remained the same as they increased in absolute intensity, up to the time (typically approximately 6 min) that some products began to be extended a second time (Figure 4 and data not shown). (The enzyme concentrations for the transition from apparent two-hit to one-hit kinetics at successive dilutions of each of the three polymerases, as assayed at fixed DNA concentrations and reaction times, should depend on the protein concentrations and the fractions of proteins which are active. For 2.5 nM context *I* (undamaged) template−primer complex, 3-min extension patterns showed transition points at 1.25 nM AtPolη, 0.31 nM HsPolη, and 0.62 nM ScPolη. Since all of these transition concentrations were substantially lower than the DNA substrate concentration, none of the polymerase preparations appear to contain large amounts of inactive protein.)

We first compared apparent insertion probabilities (defined in the legend of Figure 3) for standing-start addition of the first (here $N - 1$) nucleotide to ($N - 2$)-ended synthetic primers. Standing-start insertion depends on both the ability to bind productively to the synthetic primer and the ability to insert, so true insertion probabilities are not measured. (See the more extended discussion of this point below in Insertion Opposite Template Nucleotides 3′ to T[CPD]Ts.) However, the apparent insertion probabilities provide approximate measures of intrinsic polymerase activities. Table 2A thus suggests that specific activities (at least when measured with these primers) for contexts *I* and *II* are reasonably similar among all three polymerases but for contexts *III* and *IV* are higher for AtPolη and lower for ScPolη.

These highly nonprocessive polymerases presumably dissociate more-or-less stochastically from primers opposite undamaged templates, but local sequence context and polymerase properties may modulate dissociation rates. We quantitatively measured probabilities of termination (polymerase dissociation; defined in the legend of Figure 3) opposite template nucleotides $N - 1$, $N3'$, $N5'$, and $N + 1$ during extension of ($N - 2$)-ended synthetic primers by the three polymerases, for four different sequence contexts.

Termination probabilities were strongly affected by sequence context and nucleotide position and, in some cases, varied dramatically among the polymerases (Table 2B and Figure 5). For example, variations in $N5'$ termination probability were high for AtPolη and ScPolη but low for HsPolη [standard deviations of 52, 27, and 8%, respectively, from mean $N5'$ termination probabilities (data not shown)]. For contexts *I* and *II*, termination probabilities were roughly in the following order: ScPolη > AtPolη ≈ HsPolη. For contexts *III* and *IV*, the order was as follows: ScPolη > AtPolη > HsPolη. The very strong $N5'$ and $N + 1$ termination by ScPolη in contexts *III* and *IV* causes its primary-extension patterns to appear highly nonprocessive (see single-hit patterns in Figure 2 of the Supporting Information, for example), even though ScPolη specific activities [concentration-normalized standing-start ($N - 1$) insertion probability] were similar to those of AtPolη and HsPolη (Tables 1 and 2A).

Table 2: Kinetic Parameters on Undamaged Templates

(A) $N - 1$ Insertion[a,b]

context	AtPolη	HsPolη	ScPolη
I	0.45	0.95	0.58
II	0.41	0.86	0.67
III	0.48	1.0	0.36
IV	0.56	1.1	0.34
mean	0.47 ± 0.05	1.0 ± 0.04	0.56 ± 0.13

(B) Termination Probabilities[c]

	context	$N - 1$	$N3'$	$N5'$	$N + 1$	mean[d]	SD
AtPolη	*I*	0.45	0.41	0.44	0.47	0.47	±0.1
	II	0.41	0.42	0.3	0.46	0.39	±0.09
	III	0.36	0.62	0.81	0.98	0.6	±0.25
	IV	0.32	0.57	0.75	0.6	0.55	±0.26
HsPolη	*I*	0.47	0.41	0.34	0.56	0.43	±0.04
	II	0.53	0.51	0.26	0.61	0.48	±0.11
	III	0.35	0.34	0.38	0.48	0.37	±0.08
	IV	0.31	0.34	0.43	0.48	0.37	±0.1
ScPolη	*I*	0.58	0.74	0.84	0.84	0.71	±0.14
	II	0.73	0.84	0.45	0.58	0.63	±0.11
	III	0.66	0.78	0.4	0.95	0.75	±0.2
	IV	0.42	0.7	0.78	0.82	0.77	±0.27

[a] Undamaged template strands were paired with 18-mer ($N - 3$) primers [3′-OH thymine opposite the third template base 3′ to TT (see Figure 3)]. Primer-extension reactions were performed as described in Materials and Methods using 150 nM primer−template. [b] For comparisons of relative specific activities, normalized means were determined by dividing insertion by input protein and normalizing to HsPolη. [c] Undamaged template strands were paired with 19-mer ($N - 2$) primers [3′-OH thymine opposite the second template adenine 3′ to TT (see Figure 3)]. Primer-extension reactions were performed as described above. Termination probabilities for each template position were calculated. [d] Mean values for termination probability across template positions ($N - 1$) to ($N + 1$) in contexts *I*−*IV*.

In each context, the standard deviations (SDs) in termination probability from position to position (Table 2B, column 6) were low for HsPolη for all contexts and relatively low for AtPolη and ScPolη for contexts *I* and *II*. Interestingly, the high position-to-position variations in AtPolη and ScPolη termination for contexts *III* and *IV* (SDs of 0.20–0.27) paralleled their generally higher mean termination probabilities (primary data to support Figure 5 and Table 2 appear in Table 1 of the Supporting Information).

Extension of Primers past Template T[CPD]T Photoproducts. We compared the abilities of the three polymerases to make the three running-start insertions, opposite and immediately after T[CPD]T template nucleotides ($N3'$, $N5'$, and $N + 1$) that define CPD [1]bypass. Figure 6 shows representative experiments using synthetic $N - 2$ primers paired with undamaged (T-T) or T[CPD]T context *I* templates. Figures 7−9 show complete sets of probabilities of running-start $N3'$, $N5'$, and $N + 1$ insertions opposite T[CPD]T and undamaged (T-T) templates. Insertions opposite the $N3'$ nucleotide of T[CPD]T (Figure 7A) by AtPolη and HsPolη were both robust (probabilities of 0.5–0.8 for the various contexts), but probabilities of this $N3'$ insertion by ScPolη appeared to be considerably lower (0.02–0.12). These dramatic differences in $N3'$ insertion opposite T[CPD]T contrasted with roughly similar insertion opposite undamaged $N3'$ (Figure 7B) and similar specific activities for standing-start $N - 1$ insertion (Tables 1 and 2A).

The level of running-start $N5'$ insertion (Figure 8A) opposite T[CPD]T in all four contexts (Figure 8A) was

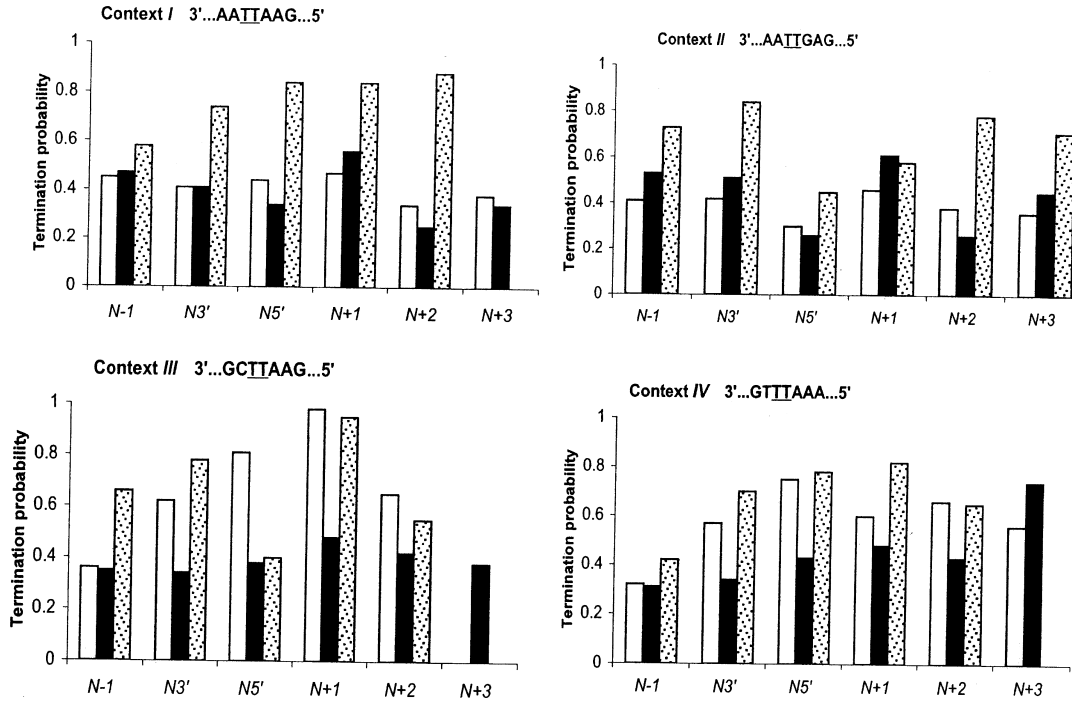

FIGURE 5: Termination opposite various nucleotides in undamaged templates. Extension of substrates (150 nM) in which ($N - 2$)-ended synthetic primers are paired with templates containing ($N5'N3'$)-TT in the indicated contexts by AtPolη (white bars; 7.5 nM), HsPolη (black bars; 3 nM), or ScPolη (stippled bars; 4.1 nM) was performed as described in the legend of Figure 4. Termination probabilities, defined in Figure 3, were determined as described in Analysis of Primer-Extension Data. Note that context sequences are shown 3′−5′, to correspond to the left-to-right direction of extension, and underlined T-T marks the $N3'N5'$ positions.

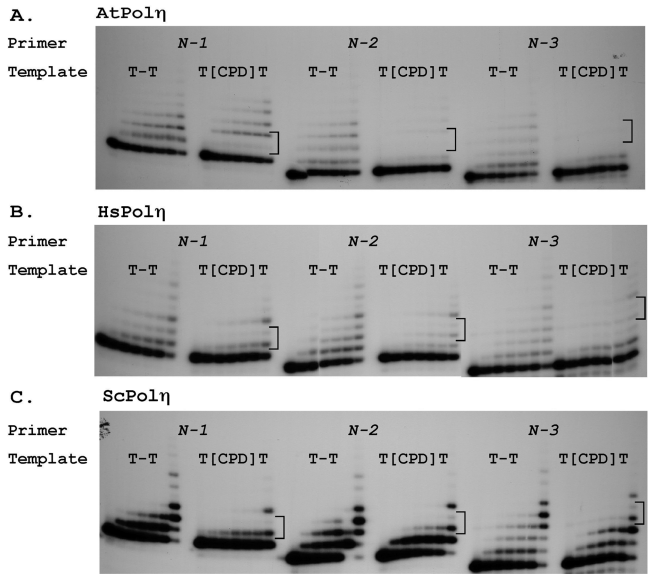

FIGURE 6: Representative extensions of various primers past T-T (undamaged) and T[CPD]T templates. Extension of indicated primers paired with indicated context *I* templates (150 nM) by AtPolη (7.5 nM), HsPolη (3.0 nM), or ScPolη (4.1 nM) was essentially as described in the legend of Figure 4. Lanes in each case correspond (from left to right) to incubations for 0, 1, 2, 3, 4, 5, and 15 min. Template nucleotides are designated according to Figure 3: T[CPD]T (indicated with a bracket) or T-T at position $N3'N5'$; template nucleotides extending 3′-wards at $N - 1$, $N - 2$, $N - 3$, etc.; nucleotides extending 5′-wards at $N + 1$, $N + 2$, etc. Synthetic primers designated according to the template nucleotides opposite their terminal (3′-OH) nucleotides correspond in each case to the lowest dark bands; very faint lower bands correspond to low-level primer impurities.

similarly high by AtPolη and HsPolη but lower by ScPolη, especially for contexts *III* and *IV*. Effects of context on $N5'$ insertion opposite undamaged (T-T) templates (Figure 8B) were less dramatic.

The final step in CPD bypass, running-start $N + 1$ insertion, was markedly context-dependent (Figure 9B). For templates with T[CPD]T in contexts *I* and *II* (Figure 9A), $N + 1$ insertions by all three polymerases were roughly similar (probabilities of 0.34–0.78). For T[CPD]T templates *III* and *IV*, however, $N + 1$ insertion probabilities were intermediate for HsPolη and low for AtPolη. The barely detectable $N + 1$ insertion by ScPolη paralleled the low $N + 1$ insertion opposite undamaged context *III* and context *IV* templates.

Complete bypasses of CPDs (insertions $N3'$, $N5'$, and $N + 1$) by the three polymerases are compared in Figure 10A. Bypass by ScPolη appeared inefficient here, reflecting quite low $N3'$ and $N5'$ insertions in all contexts, especially contexts *III* and *IV* (Figures 7A and 8A), and poor $N + 1$ insertion in contexts *III* and *IV* (Figure 10A). AtPolη bypassed T[CPD]T in contexts *I* and *II* well but bypassed T[CPD]T in contexts *III* and *IV* less efficiently. HsPolη bypassed T[CPD]T uniformly well. Dividing T[CPD]T bypass probabilities by T-T "bypass" probabilities (Figure 10B) yields apparent bypass efficiencies (Figure 10C). In most cases, AtPolη and HsPolη synthesized DNA past T[CPD]T as efficiently as past T-T or more so (apparent bypass efficiencies mostly ≥1.0). However, for these contexts, apparent ScPolη bypass efficiencies were less than 1.0.

Extension of Primers past Template [6-4] Photoproducts. We also evaluated the ability of the three polymerases to bypass template [6-4] photoproducts in contexts *III* and *IV*. While no significant complete bypass (successive $N3'$, $N5'$, and $N + 1$ insertion) past [6-4]s in either context was detected for any polymerase (Figure 3 of the Supporting Information), running-start $N3'$ insertion opposite the 3′ thymine of T[6-4]T in context *IV* was substantial for HsPolη (probability of

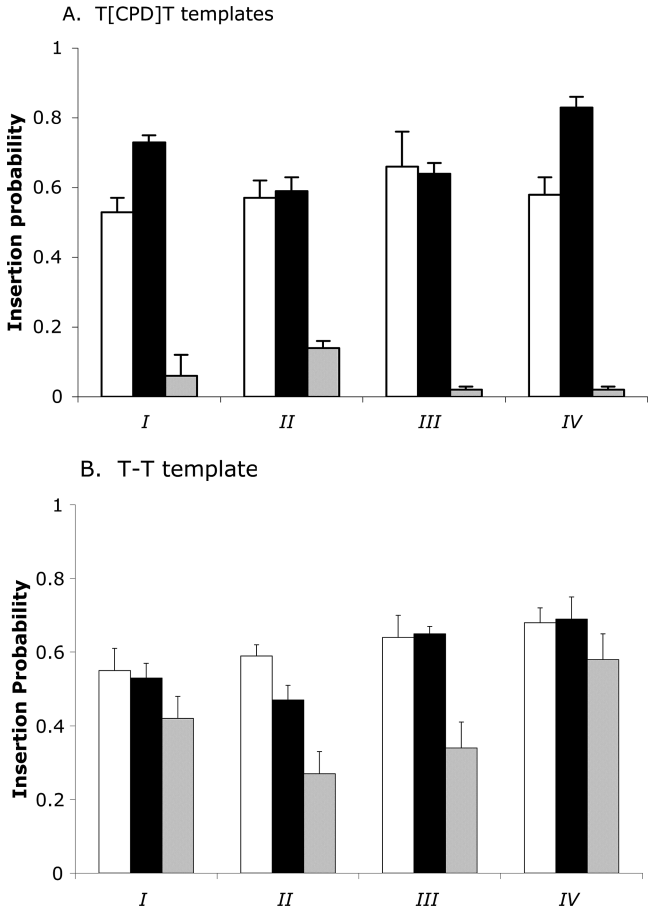

FIGURE 7: Insertion opposite 3′ nucleotides of template T[CPD]T. Extension of ($N-2$)-ended synthetic primers paired with templates containing T[CPD]T (A) or T-T (B) at *N*5′*N*3′ positions in contexts *I*−*IV* were performed under single-hit kinetic conditions, as described in the legend of Figure 5. Probabilities of running-start insertion opposite *N*3′ by AtPolη (white bars; 7.5 nM), HsPolη (black bars; 3.0 nM), or ScPolη (stippled bars; 4.1 nM), as defined in Figure 3, were determined as described in Analysis of Primer-extension Data. All primer−templates were at 150 nM.

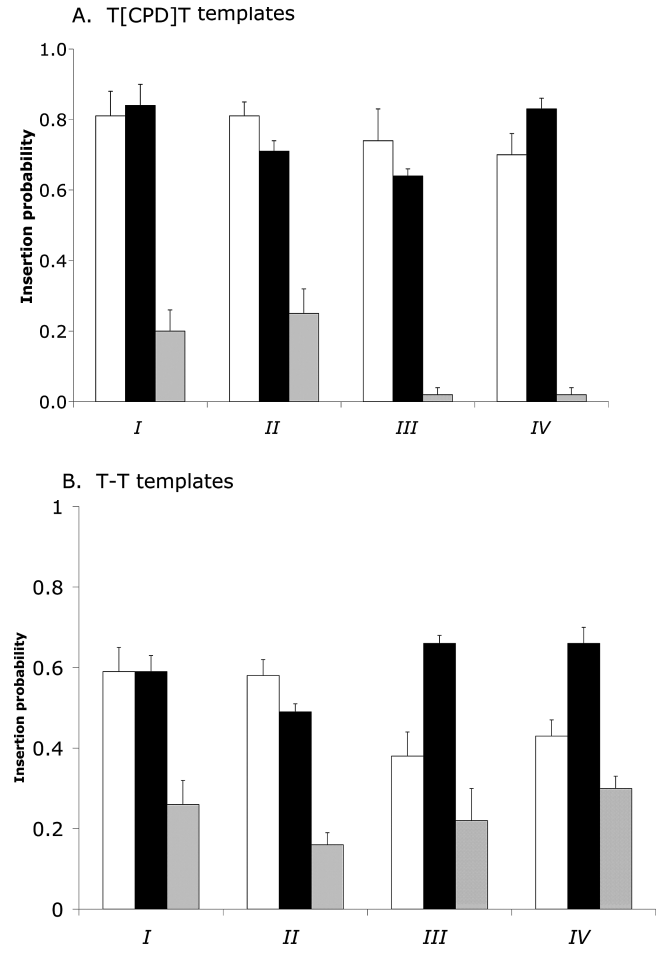

FIGURE 8: Insertion opposite 5′ nucleotides of template T[CPD]T. Extensions of ($N-2$)-ended synthetic primers paired with (*N*5′*N*3′)-T[CPD]T (A) or T-T (B) templates by AtPolη (white bars), HsPolη (black bars), or ScPolη (stippled bars) as described in the legend of Figure 7 were used to determine probabilities of running-start insertion opposite the *N*5′ template nucleotides in contexts *I*−*IV*.

0.30 ± 0.02), moderate for AtPolη (0.16 ± 0.04), and low for ScPolη. In contrast, *N*3′ insertion opposite context *IV* T[6-4]T was uniformly low (range from 0.06 to <0.02) by all three polymerases. There was no significant *N*5′ insertion by any polymerase opposite T[6-4]T in either context, as previously reported for HsPolη and ScPolη (*13*).

Insertion Opposite Template Nucleotides 3′ to T[CPD]Ts. AtPolη and HsPolη made standing-start insertions opposite the undamaged $N-1$ nucleotides just preceding (3′ to) T[CPD]T photoproducts less efficiently than opposite $N-1$ nucleotides in undamaged (T-T) templates (in Figure 6, compare $N-1$ bands for T-T vs T[CPD]T templates for AtPolη and HsPolη). For standing-start insertion, the insertion probability formula shown in Figure 3 cannot be used: the relative fraction of unextended primers (ending opposite $N-2$ template nucleotides in this case) constantly decreases, so not all band intensities remain in the same proportion to one another during the reaction time course.

If there is a constant probability of standing-start ($N-1$) insertion, such that in a small time interval dt a fraction k(dt) of the primers are extended, then unextended primers will show an exponential decrease with time. This proves to be the case for all three polymerases for context *II* T[CPD]T and T-T templates (Figure 11) and in a similar fashion for contexts *I*, *III*, and *IV* (data not shown). The pseudo-first-order rate constant k depends on the polymerase concentrations and specific activities as well as on the intrinsic microscopic probabilities for binding to primer−template and for insertion (*14*). Normalization of the respective pseudo-first-order rate constants for undamaged templates by the enzyme concentrations (Figure 11 and Figure 11 legends) (triangles) shows the relative specific activities for AtPolη, HsPolη, and ScPolη to be in the ratio 1:1.6:1.2. This is in approximate agreement with specific activities measured in a slightly different way (Tables 1 and 2A) and again shows the three intrinsic polymerase activities to be roughly similar.

Table 3 compares the $N-1$ standing-start rate constant ratios for templates with T[CPD]T versus T-T at *N*3′*N*5′ positions; the ratios should be independent of the respective polymerase concentrations and intrinsic activities. For context *I* and context *II* templates, the AtPolη and HsPolη rate constants for T[CPD]T were depressed by 63−74%, relative to the rate constants for T-T templates. ScPolη exhibited little or no such depression. For context *III* and context *IV*, the AtPolη rate constants were depressed similarly, by 60 and 75%, respectively. However, HsPolη $N-1$ insertion was depressed only by context *IV* T[CPD]T (only 38%), and ScPolη $N-1$ insertion was now also depressed (only 42 and 51%) by T[CPD]T in contexts *III* and *IV*, respectively.

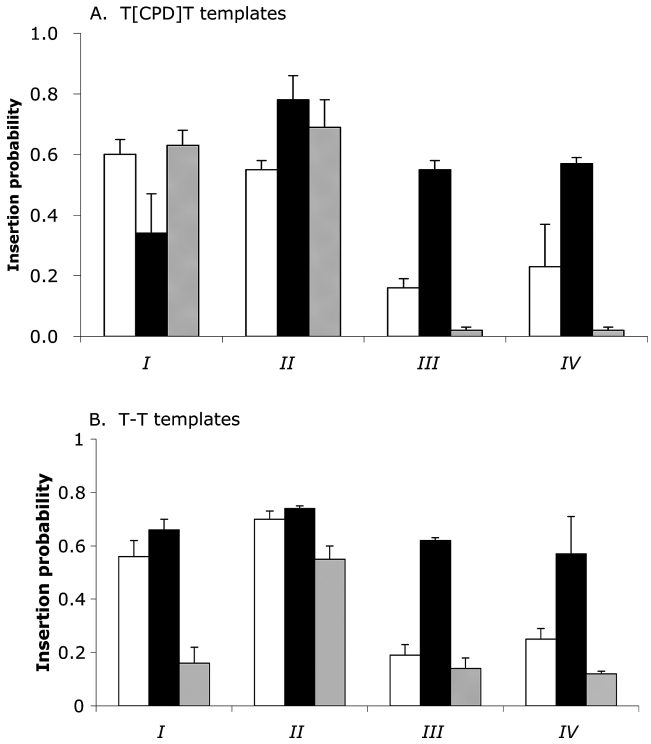

FIGURE 9: Extension of primers ending opposite photoproduct nucleotides. Extensions of synthetic ($N - 2$)-ended primers paired with templates containing T[CPD]T (A) or T-T (B) in templates *I*–*IV* by AtPolη (white bars), HsPolη (black bars), or ScPolη (stippled bars) described in the legend of Figure 7 were analyzed to obtain probabilities of $N + 1$ running-start insertion.

This "looking-ahead" effect is not due to other alterations in the T[CPD]T template DNAs: treatment of T[CPD]T-template primers with *E. coli* photolyase restored AtPolη and HsPolη standing-start $N - 1$ insertion activities to undamaged template levels for context *II* (Figure 11) and context *I* (not shown). To determine whether this effect on standing-start $N - 1$ insertion extended farther 3′ to T[CPD]Ts, we similarly analyzed standing-start $N - 2$ insertion [extension of ($N - 3$)-ended primers]. Table 3 shows modest (36–39%) depression of standing-start $N - 1$ insertion by AtPolη and HsPolη for templates containing T[CPD]T in contexts *I* and *II* but no depression of standing-start $N - 2$ insertion by ScPolη. Thus, looking-ahead effects of template T[CPD]Ts on standing-start insertion upstream by AtPolη and HsPolη extend two nucleotides 3′ to T[CPD]T, in contexts *I* and *II* at least.

The efficiency of standing-start insertion will in general depend on the probability of polymerase binding to the primer−template and on the probability of insertion by the bound polymerase (corresponding to running-start insertion probabilities). To determine which of these might be the dominant factor in depression of AtPolη and HsPolη standing-start $N - 1$ insertion by downstream (*N*3′ *N*5′) T[CPD]Ts, we analyzed running-start $N - 1$ insertion using primers ending opposite $N - 3$ template nucleotides. These running-start insertion probabilities are determined from single-hit primer-extension patterns, which remain constant during the first 4–5 min (Figure 4). Table 3 shows running-start $N - 1$ insertion by AtPolη and HsPolη to be only modestly depressed by context *II* T[CPD]T relative to T-T (15–24%); ScPolη showed almost no depression. Remarkably, running-start $N - 1$ insertion by AtPolη was 1.5-fold

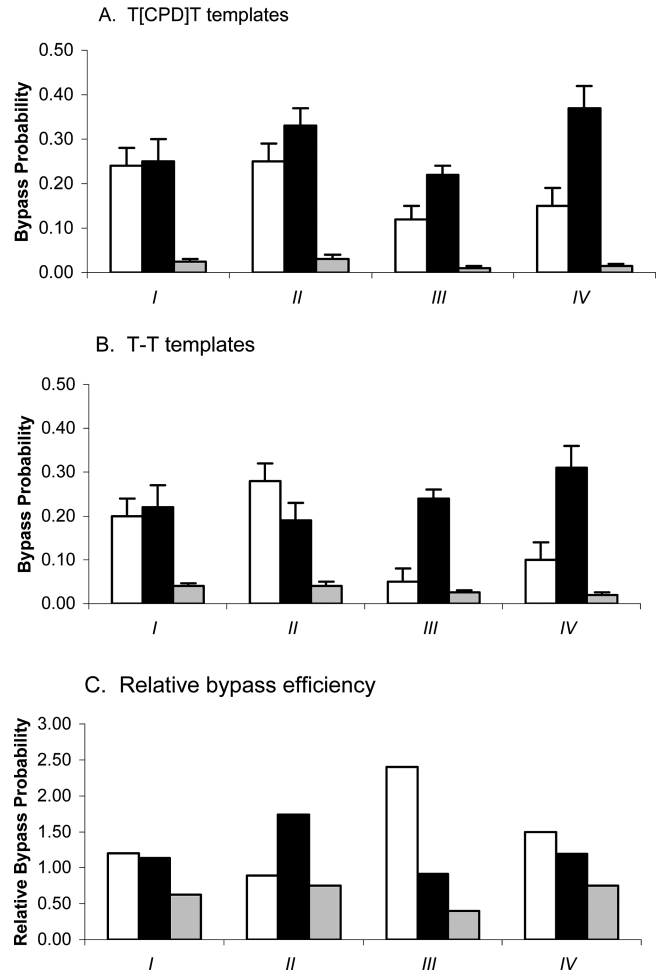

FIGURE 10: Complete bypass of template T[CPD]T. Extensions of ($N - 2$)-ended synthetic primers with templates containing T[CPD]T (A) or T-T (B) in contexts *I*–*IV* by AtPolη (white bars), HsPolη (black bars), or ScPolη (stippled bars) described in the legend of Figure 7 were analyzed to determine overall bypass probabilities [successive *N*3′, *N*5′, and $N + 1$ running-start insertions (see Figure 3)], as described in Analysis of Primer-Extension Data. Panel C shows apparent efficiencies of T[CPD]T bypass relative to T-T bypass.

higher for T[CPD]T than for T-T context *I* templates, yet the AtPolη standing-start $N - 1$ insertion was 3-fold lower for (*N*3′ *N*5′) T[CPD]T than for T-T templates. Thus, the reduced probabilities of standing-start $N - 1$ insertions by AtPolη and HsPolη (opposite template nucleotides just 3′ to T[CPD]Ts) appear to mostly reflect weakened binding to the synthetic ($N - 2$)-ended primers.

We also measured standing-start $N - 1$ insertion using templates with T[6-4]T photoproducts at *N*3′ *N*5′ positions (data not shown). Interestingly, context *III* T[6-4]T had no effect on standing-start $N - 1$ insertion by any polymerase, and context *IV* T[6-4]T depressed $N - 1$ insertion by AtPolη modestly (52%) and insertion by HsPolη only slightly (5%). However, both T[6-4]T and T[CPD]T in context *IV* substantially depressed $N - 1$ insertion by ScPolη (51 and 59%, respectively).

Insertion Opposite Undamaged Template Nucleotides beyond Photoproducts. Kunkel and co-workers (*15*) showed probabilities of termination by HsPolη to be relatively low opposite template T[CPD]T (particularly opposite position *N*5′) and/or the first ($N + 1$) undamaged nucleotide 5′ to

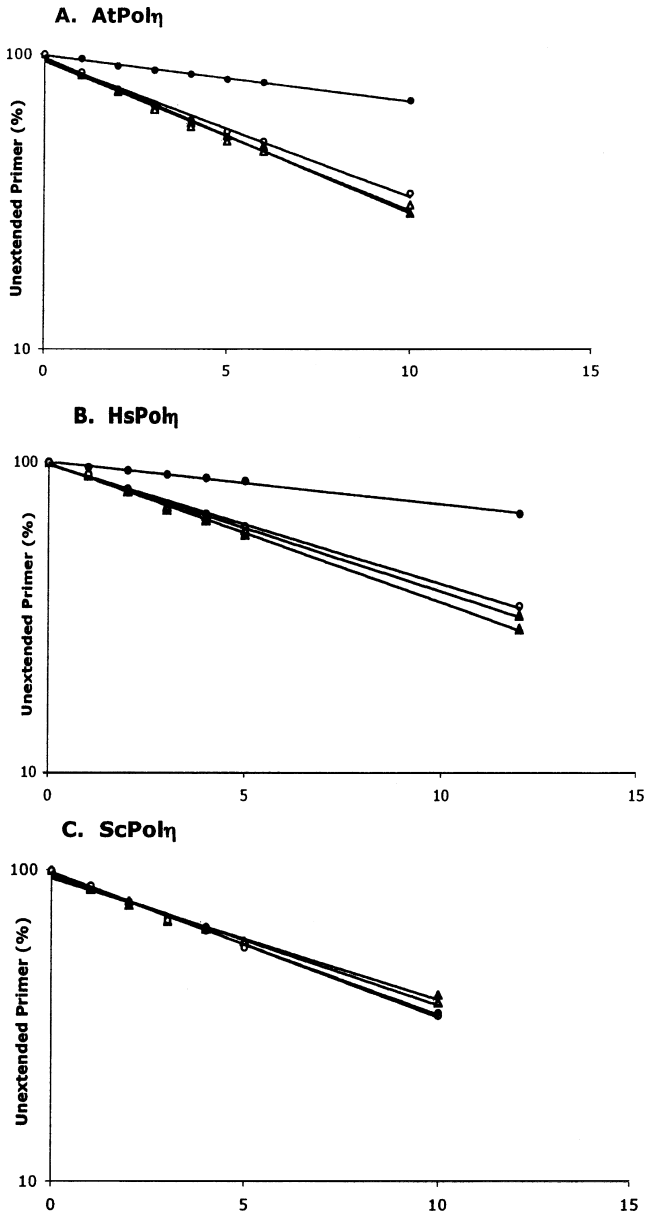

FIGURE 11: Representative standing-start insertions opposite template nucleotides immediately preceding (3′ to) T[CPD]T or T-T. $N - 1$ synthetic primers were paired with context *II* templates containing T-T (▲ and △) or T[CPD]T (● and ○). Template−primers were used directly (▲ and ●) for primer extension under single-hit conditions by AtPolη (A), HsPolη (B), or ScPolη (C) as described in Single-Hit Kinetics or used after treatment with *E. coli* CPD-photolyase plus light (△ and ○). Semilog plots of the fraction of unextended primer vs time were analyzed using Excel to determine the pseudo-first-order rate constants used to calculate the ratios listed in Table 3. Values normalized for relative protein concentration give an At:Hs:Sc ratio of 1:1.6:1.2.

T[CPD]T but substantially higher opposite the downstream nucleotides (here $N + 2$, $N + 3$, ...). They suggested that HsPolη might switch from a more processive low-termination to less processive high-termination mode once T[CPD]T bypass is completed. Binding studies by Hanaoka and coworkers support a similar inference (*14*). In vivo, this switch might facilitate replacement of error-prone Polη by a replicative polymerase. Here, such "off-switching" by HsPolη appeared to be highly context-dependent (Figure 12, black bars). In contexts *I* and *II*, the HsPolη $N + 2$ termination probabilities were 3.0 and 2.3 times the $N + 1$ probabilities, respectively, but for contexts *III* and *IV*, the HsPolη termination probabilities actually decreased slightly going from $N + 1$ to $N + 2$. For context *III*, HsPolη did show two modest switches (increases in termination probability) elsewhere, *N*5′ to $N + 1$ (1.5-fold) and $N + 2$ to $N + 3$ (1.4-fold). For context *IV*, HsPolη showed only a small *N*5′ to $N + 1$ switch (1.2-fold). AtPolη (Figure 12, white bars) showed modest $N + 1$ to $N + 2$ off-switches in contexts *I* and *II* (1.8- and 1.2-fold, respectively) and a modest *N*5′ to $N + 1$ off-switch in context *IV*. For contexts *III* and *IV*, AtPolη termination probabilities opposite $N + 1$ versus $N + 2$ were nearly the same. ScPolη showed a modest (1.5-fold) *N*5′ to $N + 1$ increase in context *II*, successive *N*5′ to $N + 1$ to $N + 2$ increases of 1.3- and 1.45-fold for context *I*, respectively, and no appreciable off-switches in contexts *III* and *IV*. Thus, the data here suggest post-CPD off-switches to be generally modest, but more substantial for HsPolη in some contexts. A similar (roughly 1.6-fold) increase in the probability of termination by ScPolη at *N*5′ versus $N + 1$ for a template incorporating T[CPD]T in a different context was recently reported (*16*).

DISCUSSION

We have compared the intrinsic biochemical properties of DNA polymerase η proteins from budding yeast, plants, and humans, organisms whose polymerases were likely subjected to different adaptive pressures during their evolution. We overexpressed His_6-tagged AtPolη, HsPolη, and ScPolη in *E. coli* under identical conditions and purified them by similar procedures. This is the first analysis of a plant polymerase η. Consistent with the presence of several nonconservative amino acid changes in their generally conserved domains, the three proteins exhibited different temperature optima for extension of primers paired with undamaged DNA templates. The considerable differences in thermal stability (HsPolη > AtPolη > ScPolη) seem consistent with adaptation to higher temperatures in warm-blooded animals and in plants frequently exposed to solar radiation. The salt optima different modestly, but all were in a physiological range (80–110 mM), and thus considerably higher than salt concentrations used in some studies of Polη biochemistry by others. Subsequent detailed analyses of the abilities of polymerases to use undamaged template−primers and to extend primers past template CPDs in four different contexts (or past [6-4] photoproducts in two contexts) were performed at the respective optimum temperatures and salt concentrations. The most striking single observation was the very strong effect of sequence context, different in general for different polymerases and for insertion opposite different template positions. Nevertheless, comparisons among the three polymerases show some trends. First, the efficiencies of synthesis by AtPolη of DNA past template T[CPD]T and past T-T in the same context closely resembled HsPolη efficiencies, particularly for contexts *I* and *II*. Second, standing-start insertion opposite undamaged nucleotides 3′ to T[CPD]T by AtPolη and HsPolη was depressed as much as 4-fold relative to insertion opposite the same nucleotides 3′ to (undamaged) T-T, as if these polymerases were looking ahead at the downstream template T[CPD]Ts. Third, ScPolη appeard less processive when copying undamaged DNA and less able to synthesize past T[CPD]T than the other two

Table 3: Relative Probabilities of Insertion Opposite Undamaged Nucleotides Upstream of T[CPD]T vs Upstream of T-T

template nucleotide			ratio of apparent rate constants (k)[c] for standing-start insertion by indicated polymerases opposite undamaged nucleotides upstream of T[CPD]T vs T-T at positions *N*3′ and *N*5′	
opposite insertion[a]	opposite primer end[b]	context	AtPolη	HsPolη
$N-1$	$N-2$	*I*	0.31	0.37
		II	0.32	0.26
		III	0.4	1
		IV	0.56	0.4
$N-2$	$N-3$	*I*	0.52	0.63
		II	0.64	1

template nucleotide			ratio of insertion probabilities[d] for running-start insertion by indicated polymerases opposite undamaged nucleotides, upstream of T[CPD]T vs T-T at positions *N*3′ and *N*5′		
opposite insertion	opposite primer end	context	AtPolη	HsPolη	ScPolη
$N-1$	$N-3$	*I*	0.04	0.78	0.94
		II	0.76	0.85	0.96

[a] Template nucleotide opposite which insertion is measured (see Figure 3). [b] Template nucleotide opposite which synthetic primer ends (see Figure 3). Note that ($N-3$)-ended primers are used for "standing-start" insertion opposite template nucleotide $N-2$ and for running-start insertion opposite $N-1$. [c] Apparent pseudo-first-order rate constants (k) were determined from slopes of *ln* (fraction of synthetic primer not extended vs time), as described in the legend of Figure 11. The ratios k(T[CPD]T template)/k((T-T) template) are shown. All data points used were within the single-hit kinetic range as defined in Materials and Methods. [d] Probabilities of running-start insertion opposite template nucleotide $N-1$ (immediately 3′ to T[CPD]T or T-T at nucleotides *N*5′ and *N*3′) were determined from analysis of product-band electropherograms, as described in *Analysis of Primer-Extension Data* as shown in Figure 3. Ratios correspond to insertion probabilities for T-T templates. Data correspond to means for two or three repetitions, with ranges typically 5−15% of means.

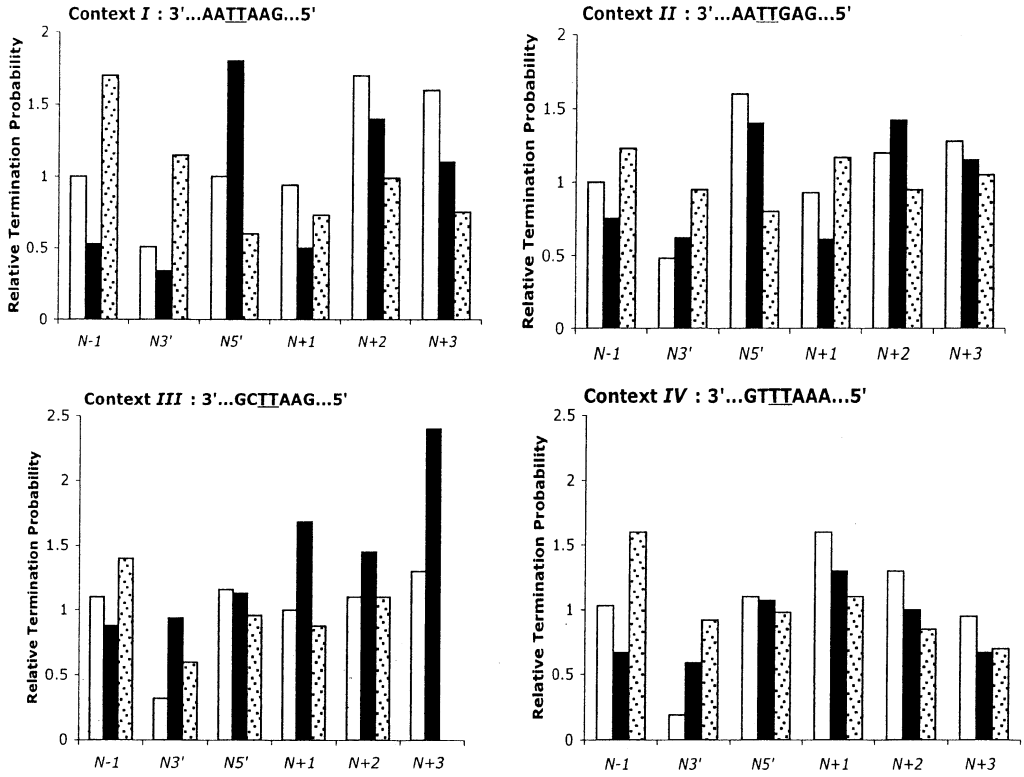

FIGURE 12: Relative efficiencies of termination opposite different template nucleotides. The extensions of synthetic ($N-2$)-ended primers paired with templates containing T[CPD]T or T-T in the indicated contexts by AtPolη (white bars), HsPolη (black bars), and ScPolη (stippled bars) described in the legend of Figure 7 were used to calculate probabilities of termination opposite the indicated template nucleotides (see Figure 3). Relative termination efficiency equals (termination probability for T[CPD]T template)/(termination probability for T-T template).

polymerases, and ScPolη did not show a consistent looking-ahead effect.

Despite the wide evolutionary separation between plants and humans, the properties of AtPolη and HsPolη analyzed here proved to be surprisingly similar, at least for contexts *I* and *II*. Both polymerases showed moderate processivity (termination probabilities were 0.4−0.6 for synthesis past undamaged T-T and the nucleotides immediately 3′ and 5′ to T-T in contexts *I* and *II*). They both synthesized DNA past T[CPD]T in these contexts as efficiently as past T-T or more so, as previously observed by others for HsPolη (*15*). These similarities between AtPolη and HsPolη with respect

to processivity and T[CPD]T bypass stand in contrast to the 3-fold difference in their specific activities (for context *I* standing-start insertion), measured at the respective salt and temperature optima. AtPolη appeared less processive than HsPolη when copying undamaged context *III* and context *IV* templates, particularly the *N*5′ nucleotide of T-T and the $N + 1$ nucleotide beyond it. AtPolη synthesized DNA past T[CPD]T in these contexts much better than past T-T. However, absolute probabilities of insertion opposite T[CPD]T templates by HsPolη were higher.

There appears to be no obvious pattern to the sequence context differences, except that only in contexts *I* and *II* are two template adenines encountered by polymerases before they encounter T[CPD]T. It remains to be determined which contexts might be most characteristic of T[CPD]Ts induced in cellular DNA.

Plants and humans thus appear to have similarly evolved polymerases able to cope well with CPDs induced by solar UV-B radiation. Humans are apparently descended from primitive mammals that lost enzymatic photoreactivation, the most efficient activity for removal of CPDs, but no fur protects human skin. Plants, by virtue of their reliance on solar radiation to drive photosynthesis, are necessarily exposed heavily to DNA-damaging UV-B wavelengths.

Some previous work utilized fusions of HsPolη to glutathione *S*-transferase (GST) or compared ScPolη purified from yeast with HsPolη expressed in insect cells. This is, to the best of our knowledge, the first comparison of similarly His_6-tagged proteins, expressed in the same organism and purified in the same manner.

Paradoxically, the robust insertion of nucleotides opposite T[CPD]T by AtPolη and HsPolη is preceded by markedly depressed standing-start insertion opposite the (undamaged) template ($N - 1$) and to a lesser extent $N - 2$ nucleotides immediately 3′ to T[CPD]T, in four (AtPolη) or three (HsPolη) contexts that were tested. Most of this looking-ahead effect appears to reflect a reduced level of binding of AtPolη and HsPolη to the ($N - 2$)-ended and ($N - 3$)-ended synthetic primers. Perhaps AtPolη and Hs Polη active sites have evolved to bind T[CPD]T−template ssDNA poorly when primers end opposite $N - 2$ and $N - 3$. Previous studies showed HsPolη binds better to substrates in which T[CPD]T templates were paired with *N*3′ synthetic primers that ended in A opposite the 3′ T than to ($N - 1$)-ended primers (*14*). However, substrates with ($N - 2$)-ended primers were not tested. Polη might be particularly error-prone at $N - 1$ positions 3′ to T[CPD]T, which could be temporarily exposed by 3′ proofreading exonucleases when replicative polymerases were stalled by template T[CPD]Ts. The looking-ahead effect would reduce the chance of error-prone $N - 1$ insertion by Polη. There was reduced but still substantial depression of even standing-start $N - 2$ insertion two nucleotides 3′ to T[CPD]T, in the two contexts that were tested. (The post-CPD "switch" to higher termination probabilities by HsPolη reported by Kunkel and co-workers (*15*) and seen here for some contexts may have similarly evolved to prevent gratuitous error-prone insertion.) A recent analysis of (relatively inefficient) bypass of 2-hydroxyadenine by truncated HsPolη (with the last 279 C-terminal amino acids missing) provides further evidence that insertion opposite an undamaged template nucleotide can be sensitive to the presence of an adjacent template lesion (*19*). In this case, running-start $N - 1$ insertion by HsPol η was dramatically lower than $N - 2$ insertion when the *N* template nucleotide was 2-hydroxyadenine, but not when the *N* nucleotide was adenine. This effect was not seen for Dpo4 polymerase or *E. coli* polymerase I Klenow fragment (lacking 3′ exonuclease).

The observed low processivity (high termination probabilities) of ScPolη versus HsPolη appears somewhat at odds with other reports (*15, 16, 27*). We consider in order these articles, none of which actually report side-by-side copying of undamaged templates by ScPolη versus HsPolη. Washington et al. (*16*) performed their analyses at 25 °C and under highly nonphysiological conditions (no salt added to the 25 mM sodium phosphate buffer). Figure 1 of the Supporting Information shows standing-start insertion by our ScPolη to be maximal at 90 mM added salt and to be reduced at least 2-fold at ≤50 mM salt. The relationship between standing-start insertion activity and processivity is not known. Nevertheless, the large effects of salt concentrations on insertion activities suggest that processivity might well also be affected. However, Washington et al. seem to have found high termination probabilities in the vicinity of undamaged T-T that roughly resemble those shown here (for different contexts) in Figure 5: their relative numbers of active polymerases decreased by 8 and 5%, respectively, during insertion opposite template nucleotide $N - 3$ to $N - 2$ to $N - 1$ (our nomenclature) but by 43, 60, and 46% during successive extensions from $N - 1$ to *N*3′ to *N*5′ to $N + 1$, respectively.

In the first report by Kunkel and co-workers (*15*), primer extension by ScPolη was assessed at 60 mM added salt, where we see a 35% reduction in intrinsic (standing-start insertion) activity (Figure 1 of the Supporting Information) and, apparently, at 37 °C, where we see a small reduction relative to that at 30 °C. Of possible concern as well is the thermal lability of ScPolη: the half-life was nearly 30 min at 35 °C (data not shown) but was only 1 min at 45 °C. We did not measure the half-life at 37 °C. The conditions used for primer extension by AtPolη in the second report by Kunkel and co-workers (*17*) were more similar to those used here (30 °C and 75 mM added salt). Besides a predicted 20% reduction in intrinsic activity (relative to that at 90 mM salt), the major difference was in the sequence surrounding T[CPD]T in their template: nine of the 10 flanking nucleotides are G or C, and a GGG run is immediately 3′ to T[CPD]T.

Thus, the conditions used for primer extension by ScPolη here and in the three studies differ significantly from one another in one or more ways. Nevertheless, the generally low ScPolη processivity seen here for DNA synthesis before, through, and beyond undamaged template T-T ($N - 1$, *N*3′, *N*5′, and $N + 1$) differs considerably from the higher ScPolη processivity reported elsewhere, although sequence contexts strongly affected the processivity. For contexts *I* and *II*, our mean ScPolη termination probabilities were 0.63, 0.73, 0.59, and 0.71, respectively, at positions $N + 1$, *N*3′, *N*5, and $N + 1$. Kunkel and co-workers (*15*) reported, for a sequence context similar to our context *I*, ScPolη termination probabilities of 0.20, 0.30, 0.49, and 0.3, respectively. For a (G+C)-rich context (*16*), the corresponding ScPolη termination probabilities are 0.50, 0.41, 0.41, and 0.21, respectively. Although Washington et al. (*27*) did not directly report

termination probabilities per se, their Figure 2B seems to show them to be 0.43, 0.60, 0.54, and 0.70, respectively.

We cannot rule out the possibility that the C-terminal His_6 tag, expression in *E. coli*, the purification procedure, or a combination of these factors may have affected ScPolη processivity. However, the intrinsic activities of the three proteins (standing-start $N - 1$ insertions) were more similar (see Tables 1 and 2A). Notably, the processivity of AtPolη, which shows the lowest intrinsic activity and requires the highest concentration to pass from single-hit to multihit kinetics (Figure 2 of the Supporting Information), was generally higher than the processivity of ScPolη. Thus, expression and purification would need to selectively depress ScPolη processivity (increase termination probabilities) but not intrinsic activity.

The higher T[CPD]T bypass efficiencies shown by AtPolη and (particularly) HsPolη versus ScPolη reflect primarily better *N*3′ and *N*5′ insertions opposite template photoproducts, rather than dramatically improved $N + 1$ extension beyond them. The modestly better insertions opposite undamaged T-T in the same contexts by AtPolη and HsPolη versus ScPolη may reflect an improved ability to deal with somewhat unstable (AT-rich) regions, perhaps indirectly contributing to improved T[CPD]T bypass. Steady-state kinetic analyses have been used to measure the catalytic efficiency k_{cat}/K_m for standing-start insertion of adenine opposite the 3′ T and 5′ T of T[CPD]T versus T-T (*17*). In general, $k_{cat}/K_m(A)$ for standing-start insertion opposite both T[CPD]T nucleotides was similar to $k_{cat}/K_m(A)$ for insertion opposite the analogous undamaged nucleotides. This was the case for both ScPolη and HsPolη, in contrast to the running-start insertion probabilities measured here (compare panel A of Figure 7 to panel B and panel A of Figure 8 to panel B). Kunkel and co-workers measured T[CPD]T bypass by ScPolη by analyzing single-hit primer-extension patterns similar to those shown (Figure 4 and Figure 2 of the Supporting Information), under somewhat different conditions (*15*). In one case, overall bypass efficiency was 100% (*16*). In the other case, however, ScPolη again made *N*3′ insertions opposite T[CPD]T as strongly as opposite T-T. However, *N*5′ insertions opposite T[CPD]T were made only 21 and 30% as well as opposite T-T, in two different contexts. $N + 1$ insertions just beyond T[CPD]T and T-T were similar for one context but were only 43% as strong opposite T[CPD]T bypass in the other context. Thus, as for processivity, the disparities between the apparently lower efficiency of T[CPD]T bypass by ScPolη versus AtPolη seen here and robust ScPolη bypass of T[CPD]T reported elsewhere may to a considerable extent reflect differences in reaction conditions and substrate DNA sequence contexts. Again, however, we cannot rule out selective inactivation of ScPolη bypass activity during expression in *E. coli* and purification. We note that homogeneous AtPolη was obtained in much lower yield (due to degradation during expression) than ScPolη and exhibited, by two criteria, lower specific activity, yet T[CPD]T bypass by AtPolη was markedly more efficient.

Two other factors, singly and/or in combination, are expected to strongly affect the consequences in vivo of the intrinsic properties of the three polymerases revealed here. First, the importance of sequence contexts cannot be overemphasized. Every activity examined here was affected by context (some more than others): termination (antiprocessivity) when copying undamaged templates, insertion opposite T[CPD]T, and insertion upstream ($N - 1$) and downstream ($N + 2$, $N + 3$) of T[CPD]T. Contexts affected some particular reactions more than others, and effects varied for different polymerases. Context differences may account for some of the disparity between the inefficient bypass of T[CPD]T by ScPolη described here versus the higher efficiency reported by Kunkel and co-workers (*16*). Interestingly, context effects on $N + 1$ insertion (extension of primers after *N*3′ and *N*5′ insertion opposite both T[CPD]T nucleotides) were generally stronger than context effects on *N*3′ and *N*5′ insertion. In several cases, yeast Polζ has proved to extend (by an $N + 1$ insertion) primers similarly "paired" with template lesions much more efficiently than the translesion polymerases that made the insertions opposite the lesions, even when Polζ itself could not make the initial insertions (reviewed in ref *20*). Thus, where particular contexts are problematic for such extensions, as in the case of T[CPD]T in contexts *III* and *IV* for AtPolη and particularly for ScPolη, Polζ may be essential for efficient bypass. This may account for some of the UV sensitivity of yeast Polζ-deficient (*rev3*) mutants (*21*). Context effects are clearly of high biological importance, but comprehensive theoretical and experimental studies are lacking. As studies of responses to T[CPD]T in more and more contexts accumulate, generalizations may emerge. Until then, detailed mechanistic interpretation of even analyses using several contexts should be viewed with caution.

Second, the intrinsic activities of Polη and some other specialized polymerases may be modified when they are attached to proliferating-cell nuclear antigen (PCNA), which appears to be monoubiquitinated during translesion synthesis (*22*). Particular insertion/termination properties might then be modified, and the effects of sequence context may be weakened. Coating of adjacent ssDNA with replication protein A (RPA) may also affect polymerase activities. Recently, ectopic expression of AtPolη in a *rad30 S. cerevisiae* mutant was reported to reverse its modest UV sensitivity (*23*). Thus, AtPolη might be able to functionally interact with yeast accessory proteins, but other explanations for the increase in UV resistance, reduction of growth rate by AtPolη expression for example, were not examined. An accompanying claim that expression of AtPolη in *E. coli* modulated UV-induced mutation spectra, suggesting AtPolη function without any eukaryotic accessory proteins, would appear to be in error. First, the authors reported that AtPolη decreased by 25% the fraction of mutations from Arg^- to Arg^+ that are due to "reversion" of an ochre codon (TAA/ATT) in *argE3* to a sense codon. They suggested that AtPolη almost always inserted A opposite T[CPD]T, whereas *E. coli* PolV occasionally generated a sense codon by inserting G. However, insertion of G opposite either the 5′ or 3′ thymine in T[CPD]T would mutate TAA to TAG or TGA, respectively. Second, the authors reported that expression of AtPolη in *E. coli* increased the level of UV-induced conversion of tRNA Gln from an amber to an ochre suppressor or tRNA Gln to an ochre suppressor de novo, by 20–30%. They suggested the primary cause of these mutations to be deamination of T[CPD]C to T[CPD]U. AtPolη was suggested to preserve the mutations by inserting AA, but *E. coli* PolV to suppress them by inserting AG. However, earlier work

by Lawrence and co-workers indicates that PolV copies both T[CPD]C and T[CPD]U quite accurately in vivo, inserting AG and AA (*24*), respectively [human Polι does frequently incorporate G opposite T (*25*), and this misinsertion tendency might extend to CPDs, especially in response to particular DNA contexts (*26*)].

Thus, the frequencies of CPD-induced mutation at particular dipyrimidine sites in various organisms may depend on the intrinsic CPD bypass properties of their particular Polη, on their modification by PCNA and RPA, and, quite strongly, on the local DNA sequence context.

ACKNOWLEDGMENT

We thank Roger Woodgate for the kind gift of UV lesion-containing oligomers and Fumio Hanaoka and Zhigang Wang for Polη expression vectors from humans and yeast, respectively. We also thank Andrew Buermeyer, Thomas Kunkel, and Roger Woodgate for helpful suggestions in the preparation of the manuscript and Buck Wilcox for help in assembling the final draft.

SUPPORTING INFORMATION AVAILABLE

Salt optimization for Polη (Figure 1), transitions from multihit to single-hit kinetics (Figure 2), extension of primers paired with templates containing T-T, T[CPD]T, or T[6-4]T (Figure 3), and three tables of extensions of primers past T-Ts, T[CPD]Ts, and T[6-4]Ts. This material is available free of charge via the Internet at http://pubs.acs.org.

REFERENCES

1. Friedberg, E. C., Wagner, R., and Radman, M. (2002) Specialized DNA polymerases cellular survival, and the genesis of mutations. *Science 296*, 1627–1630.
2. Trincao, J., Johnson, R. E., Escalante, C. R., Prakash, S., Prakash, L., and Aggarwal, A. K. (2001) Structure of the catalytic core of *S. cerevisiae* DNA polymerase η: Implications for translesion DNA synthesis. *Mol. Cell 8*, 417–426.
3. Ohmori, H., Friedberg, E. C., Fuchs, R. P., Goodman, M. F., Hanaoka, F., Hinkle, D., Kunkel, T. A., Lawrence, C. W., Livneh, Z., Nohmi, T., Prakash, L., Prakash, S., Todo, T., Walker, G. C., Wang, Z., and Woodgate, R. (2001) The Y-family of DNA polymerases. *Mol. Cell 8*, 7–8.
4. Johnson, R. E., Prakash, S., and Prakash, L. (1999) Efficient bypass of a thymine-thymine dimer by yeast DNA polymerase, Pol η. *Science 283*, 1001–1004.
5. Masutani, C., Kusomoto, A., Yamada, A., Dohmae, N., Yokoi, M., Yuasa, M., Araki, M., Iwai, S., Takio, K., and Hanaoka, F. (1999) The *XPV* (xeroderma pigmentosum variant) gene encodes human DNA polymerase η. *Nature 399*, 700–704.
6. Lehmann, A. R. (1975) Xeroderma pigmentosum cells with normal levels of excision repair have a defect in DNA synthesis after UV-irradiation. *Proc. Natl. Acad. Sci. U.S.A. 72*, 219–223.
7. Washington, M. T., Johnson, R. E., Prakash, S., and Prakash, L. (2000) Accuracy of thymine-thymine dimer bypass by *Saccharomyces cerevisiae* DNA polymerase η. *Proc. Natl. Acad. Sci. U.S.A. 97*, 3094–3099.
8. Haracska, L., Yu, S. L., Johnson, R. E., Prakash, L., and Prakash, S. (2000) Efficient and accurate replication in the presence of 7,8-dihydro-8 oxoguanine by DNA polymerase η. *Nat. Genet. 25*, 458–461.
9. Yuan, F., Zhang, Y., Rajpal, D. K., Wu, X., Guo, D., Wang, M., Taylor, J. S., and Wang, Z. (2000) Specificity of DNA lesion bypass by the yeast DNA polymerase η. *J. Biol. Chem. 275*, 8233–8239.
10. Murata, T., Iwai, S., and Ohtsuka, E. (1990) Synthesis and characterization of a substrate for T4 endonuclease V containing a phosphorodithioate linkage at the thymine dimer site. *Nucleic Acids Res. 18*, 7279–7286.
11. Kokoska, R. J., McCulloch, S. D., and Kunkel, T. A. (2003) The efficiency and specificity of apurinic/apyrimidinic site bypass by human DNA polymerase η and *Sulfolobus solfataricus* Dpo4. *J. Biol. Chem. 278*, 50537–50545.
12. Creighton, S., Bloom, L. B., and Goodman, M. F. (1995) Gel fidelity assay measuring nucleotide misinsertion, exonucleolytic proofreading, and lesion bypass efficiencies. *Methods Enzymol. 262*, 232–256.
13. Johnson, R. E., Haracska, L., Prakash, S., and Prakash, L. (2001) Role of DNA polymerase η in the bypass of a (6–4) TT photoproduct. *Mol. Cell. Biol. 21*, 3558–3563.
14. Kusumoto, R., Masutani, C., Shimmyo, S., Iwai, S., and Hanaoka, F. (2004) DNA binding properties of human DNA polymerase η: Implications for fidelity and polymerase switching of translesion synthesis. *Genes Cells 9*, 1139–1150.
15. McCulloch, S. D., Kokoska, R. J., Matsutani, C., Iwai, S., Hanaoka, F., and Kunkel, T. T. (2004) Preferential cis-syn thymine dimer bypass occurs with biased fidelity. *Nature 428*, 97–99.
16. McCulloch, S. D., Wood, A., Garg, P., Burgers, P. M., and Kunkel, T. A. (2007) Effects of accessory proteins on the bypass of a cis-syn thymine-thymine dimer by *Saccharomyces cerevisiae* DNA polymerase η. *Biochemistry 46*, 8888–8896.
17. Johnson, R. E., Washington, M. T., Haracska, L., Prakash, S., and Prakash, L. (2000) Eukaryotic polymerase [ι] and [ξ] act sequentially to bypass DNA lesions. *Nature 406*, 1015–1019.
18. McDonald, J. P., Levine, A. S., and Woodgate, R. (1997) The *Saccharomyces cerevisial RAD30* gene, a homologue of *Escherichia coli* dinB and umuC, is DNA damage inducible and functions in a novel error-free postreplication repair mechanism. *Genetics 147*, 1557–1568.
19. Barone, F., McCulloch, S. D., Macpherson, P., Maga, G., Yamada, M., Nohmi, T., Minoprio, A., Mazzei, F., Kunkel, T. A., Karran, P., and Bignami, M. (2007) Replication of 2-hydroxyadenine-containing DNA and recognition by human MutSalpha. *DNA Repair 6*, 355–366.
20. Prakash, S., Johnson, R. E., and Prakash, L. (2005) Eukaryotic translesion synthesis DNA polymerases: Specificity of structure and function. *Annu. Rev. Biochem. 74*, 317–353.
21. Lawrence, C., and Christensen, R. (1976) UV Mutagenesis in Radiation-Sensitive Strains of Yeast. *Genetics 82*, 207–232.
22. Haracska, L., Kondratick, C. M., Unk, I., Prakash, S., and Prakash, L. (2001) Interaction with PCNA is essential for yeast DNA polymerase η function. *Mol. Cell 8*, 407–415.
23. Santiago, M. J., Alejandre-Duran, E., and Ruiz-Rubio, M. (2006) Analysis of UV-induced mutation spectra in *Escherichia coli* by DNA polymerase η from *Arabidopsis thaliana*. *Mutat. Res. 601*, 51–60.
24. Horsfall, M. J., Borden, A., and Lawrence, C. W. (1997) Mutagenic properties of the T-C cyclobutane dimer. *J. Bacteriol. 179*, 2835–2839.
25. Tissier, A., McDonald, J. P., Frank, E. G., and Woodgate, R. (2000) Pol iota, a remarkably error-prone human DNA polymerase. *Genes Dev. 14*, 1642–1650.
26. Vaisman, A., Frank, E. G., Iwai, S., Ohashi, E., Ohmori, H., Hanaoka, F., and Woodgate, R. (2003) Sequence context-dependent replication of DNA templates containing UV-induced lesions by human DNA polymerase ι. *DNA Repair 2*, 991–1006.
27. Washington, M. T., Johnson, R. E., Prakash, L, and Prakash, S. (1999) Fidelilty and processivity of *Saccharomyces cerevisiae* DNA polymerase η. *J. Biol. Chem. 274*, 36835–36838.

BI701781P